

# Broadband lasing and nonlinear conversion of radiation from $\text{LiF} : F_2^+$ and $\text{LiF} : F_2^-$ colour centre lasers

V V Fedorov, P G Zverev, T T Basiev

**Abstract.** Broadband  $\text{LiF}:F_2^+$  and  $\text{LiF}:F_2^-$  colour centre lasers are studied theoretically and experimentally. The cavities of these lasers ensure spatial wavelength selection. The lasers generate nanosecond pulses in the near-infrared range with a spectrum wider than  $1300 \text{ cm}^{-1}$ . As a result of optimisation of the optical layout and selection of proper nonlinear crystals, the broadband laser radiation with a spectral width of more than  $1300 \text{ cm}^{-1}$  is efficiently and simultaneously converted into the second harmonic in a nonlinear  $\text{LiIO}_3$  crystal and into the fourth harmonic, in a nonlinear BBO crystal.

**Keywords:** colour centres, harmonic generation, broadband lasing.

## 1. Introduction

A narrow spectral lasing line is a characteristic feature of laser radiation. However, recently it has become necessary to build sources of collimated high-intensity radiation with a broad lasing spectrum or with a certain discrete spectral set of lasing lines, which can be used for scientific and technological purposes. Usually, the competition of modes in the active element with homogeneously broadened luminescence bands narrows the output radiation spectrum, which proves to be substantially narrower than a luminescence band. A possible way to achieve broadband lasing is to use cavities with spatial dispersion [1–3]. In such a laser, the lasing modes with different wavelengths propagate in different parts of the active element, which removes the competition between the modes.

$\text{LiF}$  crystals with  $F_2^+$  and  $F_2^-$  colour centres have attracted much interest as elements for broadband lasers because they produce highly efficient tunable lasing in broad spectral ranges ( $0.85\text{--}1.1 \mu\text{m}$  for  $F_2^+$  colour centres and  $1.04\text{--}1.28 \mu\text{m}$  for  $F_2^-$  colour centres [4, 5]).

In this paper, we studied a broadband  $\text{LiF}$  colour centre laser that generates pulses with a spectral width close to that of the luminescence spectrum. The laser also provides the

efficient doubling and quadrupling of the frequency of broadband infrared radiation.

## 2. Principle of operation of a broadband laser

The high concentration of active centres in the dye solution in the cavity of a broadband dye laser [1] allows one to achieve spatial dispersion by focusing the laser radiation in a thin layer of the dye. In colour centre crystal lasers operating at room temperature, the active element is usually several centimetres long [4]. Hence, to achieve broadband lasing, a special cavity is required with spatial dispersion that extends over the entire length of the active element. The schematic of such a laser is shown in Fig. 1. The laser cavity consists of the input dichroic mirror 1, the diffraction grating 5, which operates in the autocollimation regime, the intracavity lens 3, and the diaphragm 4. The laser operates as follows: the beams propagating in the active element parallel to the optical axis of the system are focused by lens 3, while the beams that propagate at a distance from the optical axis are incident on the diffraction grating (after passing through the lens) at different angles  $\theta$ . As a result, the autocollimation condition for each beam is satisfied at

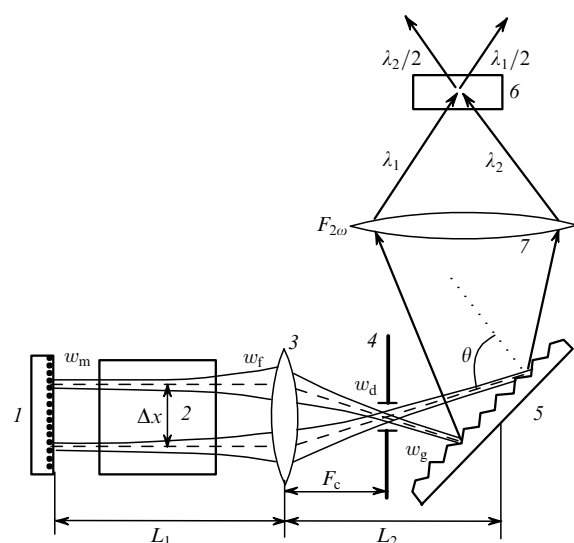


**Figure 1.** Optical schematic of the cavity of a broadband laser with a frequency doubler: (1) input dichroic mirror; (2) active element; (3) intracavity lens; (4) diaphragm; (5) diffraction grating operating in the autocollimation regime; (6) nonlinear crystal; (7) frequency doubler lens.

V V Fedorov, P G Zverev, T T Basiev Laser Materials and Technologies Research Center of General Physics Institute, Russian Academy of Sciences, Ul. Vavilova 38, 119991, GSP-1 Moscow, Russia  
Tel. (7-095) 135-0318; fax (7-095) 135-0270; e-mail: zverev@lst.gpi.ru

Received 14 November 2000

Kvantovaya Elektronika 31 (4) 285–289 (2001)

Translated by E M Yankovsky

different radiation wavelengths, which are determined by the relation

$$2d \sin \theta = m\lambda, \quad (1)$$

where  $d$  is the grating period;  $m$  is the diffraction order;  $\theta$  is the autocollimation angle;  $\lambda$  is the laser beam wavelength. The diaphragm 4 removes the 'skew' beams propagating in the active element at an angle to the optical axis of the cavity. In such a cavity, the optical paths of the beams with different wavelengths are spatially separated within the active element, which eliminates their competition and permits lasing with the spectral width close to that of luminescence.

To provide broadband lasing of  $\text{LiF} : F_2^+$  and  $\text{LiF} : F_2^-$  lasers with a  $1200\text{-mm}^{-1}$  diffraction grating operating in the first diffraction order ( $m = 1$ ) in the range from  $\lambda_1 = 0.87 \mu\text{m}$  to  $\lambda_2 = 1.1 \mu\text{m}$  and from  $\lambda_1 = 1.1 \mu\text{m}$  to  $\lambda_2 = 1.25 \mu\text{m}$ , respectively, one should excite in the active element the region of the width

$$\Delta x \approx F_c \tan[\theta(\lambda_2) - \theta(\lambda_1)], \quad (2)$$

where  $F_c$  is the focal length of the intracavity lens. For instance, to achieve broadband lasing of the  $\text{LiF} : F_2^+$  laser in the  $0.87\text{--}1.1\text{-}\mu\text{m}$  range at  $F_c = 50 \text{ mm}$ , the width  $\Delta x$  of the excited region within the active element should be  $8.5 \text{ mm}$ , while for the  $\text{LiF} : F_2^-$  laser operating in the  $1.1\text{--}1.25\text{-}\mu\text{m}$  range, it should be  $6.4 \text{ mm}$ .

The dispersion  $dx/d\lambda$  of wavelengths in the active element is determined by the dispersion  $d\theta/d\lambda$  of the diffraction grating:

$$\frac{dx}{d\lambda} = F_c \frac{d\theta}{d\lambda}. \quad (3)$$

Using the intracavity lens with  $F_c = 50 \text{ mm}$  one has the dispersion  $dx/d\lambda = 3.6 \mu\text{m} \text{ \AA}^{-1}$  for the  $\text{LiF} : F_2^+$  laser and  $4.1 \mu\text{m} \text{ \AA}^{-1}$  for the  $\text{LiF} : F_2^-$  laser.

To study the spectral resolution of a broadband laser, we estimate the size of its fundamental  $\text{TEM}_{00}$  mode in the Gaussian approximation [6]. Consider a cavity with equal arms with respect to the intracavity lens ( $L_1 = L_2 = L$ ) (Fig. 1). The distribution of the fundamental-mode field in this cavity is symmetric with respect to lens 3, and the dimensions of the waists on the flat mirror ( $w_m$ ) and the diffraction grating ( $w_g$ ) are the same:

$$w_m^2 = w_g^2 = \frac{L\lambda}{\pi} \left( \frac{2F - L}{L} \right)^{1/2}. \quad (4)$$

Dimensions of the mode on the lens ( $w_f$ ) and the diaphragm ( $w_d$ ) are

$$w_f^2 = \frac{L\lambda}{\pi} \left[ \frac{4F^2}{(2F - L)L} \right]^{1/2}, \quad w_d^2 = w_m^2 \left\{ 1 + \left[ \frac{\lambda(L - F)}{\pi w_m^2} \right]^2 \right\}. \quad (5)$$

In order to select modes with different wavelengths, diaphragm 4 is placed in the focal plane of lens 3. For a cavity of a broadband laser with parameters close to those of the real dimensions of the model ( $L = 80 \text{ mm}$  and  $F_c = 50 \text{ mm}$ ), we have (for  $\lambda = 1 \mu\text{m}$ )

$$w_m = 113 \mu\text{m}, \quad w_f = 253 \mu\text{m}, \quad w_d = 141 \mu\text{m}. \quad (6)$$

Figure 1 shows that it is preferable to place the active medium close to mirror 1, because there the size of the fundamental-mode waist and, hence, the spectral overlap of modes with different wavelengths are minimal. The spectral resolution of a broadband laser can be estimated from equation (3) as the ratio of the size  $2w_m$  of the fundamental-mode spot on the mirror to the wavelength dispersion  $dx/d\lambda$  in the active element. Estimates of the spectral width of the fundamental lasing mode for broadband  $\text{LiF} : F_2^+$  and  $\text{LiF} : F_2^-$  lasers yield

$$\delta\lambda_{F_2^+} = \frac{2w_m}{FD} \approx 63 \text{ \AA}, \quad \delta\lambda_{F_2^-} = \frac{2w_m}{FD} \approx 55 \text{ \AA}. \quad (7)$$

Thus, lasing of the broadband lasers under study (the width of the spectrum is  $230 \text{ nm}$  for the  $\text{LiF} : F_2^+$  laser and  $150 \text{ nm}$  for the  $\text{LiF} : F_2^-$  laser) can be treated as simultaneous lasing of 40 and 30 independent lasers, respectively.

### 3. Conversion of radiation from broadband colour-centre crystal lasers into the visible and UV range

In Ref. [7], frequency doubling of radiation with a spectral width of about  $10 \text{ nm}$  was obtained in a nonlinear crystal by compensating the angular matching dispersion using a prism. The spectral width of the output radiation from the  $\text{LiF} : F_2^+$  and  $\text{LiF} : F_2^-$  colour centre lasers exceeds  $100 \text{ nm}$ . The frequency doubling in such a broad spectral range requires special optimisation, i.e., the matching of the angular dispersion of the output from a broadband laser with the angular matching dispersion of a nonlinear crystal.

One of the possible ways of optimising is to change the angular magnification of lens 7 (Fig. 1). In the linear approximation, the required angular magnification  $\Gamma$  of the optical system is given by the expression

$$\Gamma = \frac{d\theta/d\lambda}{d\alpha/d\lambda}, \quad (8)$$

where  $d\alpha/d\lambda$  is the phase-matching angle dispersion at the entrance to the nonlinear crystal;  $d\theta/d\lambda$  is the dispersion of the output radiation of the broadband laser. This scheme operates efficiently only in crystals with phase-matching of the ooe or eeo type.

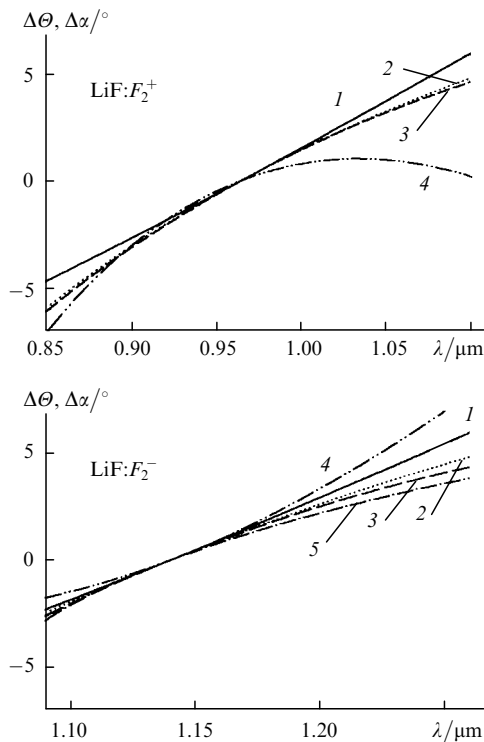
The optimal nonlinear crystal was selected by calculating the spectral dependence of the phase-matching angles for different crystals [8]. It was assumed that the crystal is cut for normal incidence of radiation at a wavelength corresponding to the middle of the spectral range of lasing (at  $0.965 \mu\text{m}$  for the  $\text{LiF} : F_2^+$  laser and at  $1.14 \mu\text{m}$  for the  $\text{LiF} : F_2^-$  laser).

Table 1 lists the calculated phase-matching angles  $\alpha_0$  with respect to the optical axis of the crystal for wavelengths of  $965$  and  $1.14 \mu\text{m}$ , the angular matching dispersion  $d\alpha/d\lambda$  outside the crystal, the nonlinearity coefficient  $D_{\text{eff}}$ , and the widths of the spectral ( $\Delta\lambda$ ), angular ( $\Delta\alpha$ ), and temperature ( $\Delta T$ ) phase-matching for some crystals.

Fig. 2 presents the calculated dispersion curves for the angle of incidence of the radiation from broadband  $\text{LiF} : F_2^+$  and  $\text{LiF} : F_2^-$  lasers on the nonlinear crystal (solid curves) and the phase-matching angles in KDP, BBO,  $\text{LiNbO}_3$ , and  $\text{LiIO}_3$  crystals recalculated with allowance for optimal angular magnification  $\Gamma$ .

**Table 1.** Parameters of nonlinear crystals (1-cm long) used for frequency doubling of broadband LiF:F<sub>2</sub><sup>+</sup> and LiF:F<sub>2</sub><sup>-</sup> lasers, and the calculated widths of the spectral ( $\Delta\lambda$ ), angular ( $\Delta\alpha$ ), and temperature ( $\Delta T$ ) phase-matchings [8].

Crystal	$\alpha_0/^\circ$		$d\alpha/d\lambda/^\circ \mu\text{m}^{-1}$		$\Delta\lambda/\text{nm}$	$\Delta\alpha/\text{mrad}$	$\Delta T/^\circ\text{C}$	$D_{\text{eff}}/10^{-12} \text{ m V}^{-1}$
	0.965 $\mu\text{m}$	1.14 $\mu\text{m}$	0.965 $\mu\text{m}$	1.14 $\mu\text{m}$				
KDP	41.4	41.7	11	15	28.3	1.7	25.1	0.29
LiIO <sub>3</sub>	33.5	27.9	75	45	0.7	0.6	–	2.75
LiNbO <sub>3</sub>	–	69.3	–	240	0.3	3.1	1.1	5.32
BBO	24.5	22.8	33	17	2.1	0.52	39.8	1.69–2.1

**Figure 2.** Calculated dispersion dependences for the angle of incidence  $\Theta = 90^\circ - \Delta\Theta$  of the radiation from broadband LiF : F<sub>2</sub><sup>+</sup> and LiF : F<sub>2</sub><sup>-</sup> lasers on the nonlinear crystal (1) and for the phase-matching angle  $\alpha = \Delta\alpha + \alpha_0$  for frequency doubling in the LiIO<sub>3</sub> (2), BBO (3), KDP (4), and LiNbO<sub>3</sub> (5) crystals.

Among the nonlinear crystals considered, LiNbO<sub>3</sub> has the largest nonlinearity coefficient ( $D_{\text{eff}} = 5.32 \times 10^{-12} \text{ m V}^{-1}$ ). This crystal exhibits a strong nonlinear dependence of the phase-matching angle on the wavelength, which makes it possible to obtain  $90^\circ$  phase-matching by decreasing the wavelength to 1.05  $\mu\text{m}$ . Hence, this crystal is suitable only for doubling the output frequency of the LiF : F<sub>2</sub><sup>-</sup> laser. However, the strong nonlinearity leads to a substantial discrepancy between the angular matching curves and the wavelength dependence of the angle of incidence of the radiation from a broadband laser on the nonlinear crystal (angular mismatch). The dispersion dependence of the

phase-matching angle of the KDP crystal has a flat maximum around 1.05  $\mu\text{m}$ . As a result, strong angular mismatch was observed for the LiF : F<sub>2</sub><sup>+</sup> laser.

The KDP crystal has the smallest nonlinearity coefficient ( $D_{\text{eff}} = 0.29 \times 10^{-12} \text{ m V}^{-1}$ ) among the crystals we studied. The spectral dependences of the phase-matching angles for the LiIO<sub>3</sub> and BBO crystals are similar (Fig. 2) when the angular magnifications  $\Gamma$  are optimal ( $\Gamma_{\text{BBO}} = 0.8$  and  $\Gamma_{\text{LiIO}_3} = 1.8$  for the 0.87–1.1- $\mu\text{m}$  range, and  $\Gamma_{\text{BBO}} = 0.4$  and  $\Gamma_{\text{LiIO}_3} = 1$  for the 1.1–1.25- $\mu\text{m}$  range). The LiIO<sub>3</sub> crystal has a somewhat better angular matching and a larger nonlinearity coefficient ( $D_{\text{eff}} = 2.75 \times 10^{-12} \text{ m V}^{-1}$ ) compared to the BBO crystal ( $D_{\text{eff}} = (1.69 - 2.1) \times 10^{-12} \text{ m V}^{-1}$ ). Thus, among the crystals we examined the LiIO<sub>3</sub> crystal proved to be the best for frequency doubling of the infrared radiation emitted by a broadband laser.

The broadband radiation produced in the visible region can be converted into the UV range by doubling its frequency once more. After the frequency doubling in a nonlinear crystal with the ooe phase-matching, the polarisation of the second-harmonic radiation lies in the diffraction plane of the grating. For further conversion of the radiation to the fourth harmonic, the polarization of the second harmonic of the broadband radiation should be rotated  $90^\circ$  using, for example, an optically active quartz crystal.

Table 2 lists the parameters of the KDP and BBO crystals used for conversion of broadband radiation to the fourth harmonic. These crystals have approximated the same spectral dependences of the phase-matching angle. The width of angular matching in KDP is twice as large as in BBO, but the latter has a nonlinearity coefficient that is three times as large as that of the former and ensures better angular matching. In view of this, BBO is the most efficient nonlinear crystal for generating the fourth harmonic from a broadband laser.

#### 4. Experimental results

We studied broadband LiF : F<sub>2</sub><sup>+</sup> and LiF : F<sub>2</sub><sup>-</sup> lasers whose output radiation frequency was doubled and quadrupled. The schematic of this laser is similar to that shown in Fig. 1. Cylindrical lenses with focal lengths  $F_c = 30$  and 50 mm were used as the intracavity lens. The 1200- $\text{mm}^{-1}$  diffraction grating operated in the autocollimation regime in the first diffraction order. The pump radiation was focused in the vertical plane by a cylindrical lens with

**Table 2.** Calculated parameters of nonlinear crystals (1-cm long) used for the fourth harmonic generation of a broadband LiF:F<sub>2</sub><sup>-</sup> laser, and the widths of the spectral ( $\Delta\lambda$ ), angular ( $\Delta\alpha$ ), and temperature ( $\Delta T$ ) phase-matchings [8].

Crystal	$\alpha_0/^\circ$	$d\alpha/d\lambda/^\circ \mu\text{m}^{-1}$	$\Delta\lambda/\text{nm}$	$\Delta\alpha/\text{mrad}$	$\Delta T/^\circ\text{C}$	$D_{\text{eff}}/10^{-12} \text{ m V}^{-1}$
KDP	76.6	30	0.13	1.6	1.2	0.45
BBO	47.4	41	0.07	0.16	5.4	1.29–1.62

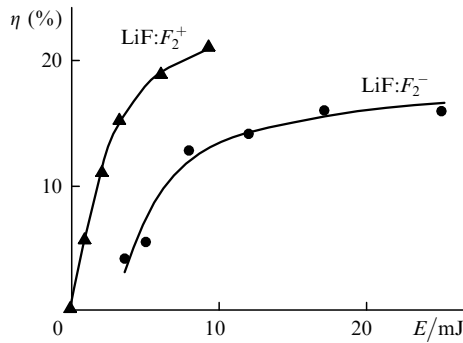


**Figure 3.** Dependences of the efficiency  $\eta$  of broadband lasing of  $\text{LiF:F}_2^+$  and  $\text{LiF:F}_2^-$  crystal lasers on the pump laser energy  $E$ .

$F_c = 120$  mm and was coupled to the cavity through a dichroic mirror. The spectrum of the broadband radiation was detected (per lasing pulse) by a BM-25 polychromator coupled with a diode array or a digital camera. The averaged lasing spectra were recorded with an MDR-23 monochromator coupled with a photodiode, and a gated integrator. The active elements used in the experiments were LiF crystals 4-cm long cut at the Brewster angle. The high concentration of stable laser-active  $F_2^-$  and  $F_2^+$  colour centres in LiF crystals was produced upon irradiation of the crystals.

A pulsed 1.047- $\mu\text{m}$   $Q$ -switched  $\text{Nd}^{3+} : \text{YLiF}$  laser operating with a pulse repetition rate of 10–50 Hz was used to excite the broadband  $\text{LiF} : F_2^-$  laser. The absorption coefficient of the  $\text{LiF} : F_2^-$  crystal at the pump wavelength was  $K_{1.047} = 0.7 \text{ cm}^{-1}$ . In Ref. [9], it was shown that pumping by a  $\text{Nd}^{3+} : \text{YLiF}$  laser (with a shorter wavelength), provides the efficiency of the  $\text{LiF} : F_2^-$  laser that is twice as high as upon pumping by a  $\text{Nd}^{3+} : \text{YAG}$  laser. The dependence of the overall energy efficiency of the broadband  $\text{LiF} : F_2^-$  laser on the pump energy is shown in Fig. 3. The maximum efficiency, equal to 16%, was reached at a pump energy equal to  $E = 25$  mJ and transverse dimensions of the pumped region equal to 8 mm  $\times$  1 mm. Fig. 4a shows the experimental spectrum of broadband lasing of the  $\text{LiF} : F_2^-$  laser with a width of more than 0.15  $\mu\text{m}$  in the near-infrared range (1.08–1.23  $\mu\text{m}$ ). The radiation of the broadband laser represents a continuous fan of laser beams diverging in the horizontal plane and propagating in accordance with the autocollimation condition (1). By using cylindrical lenses, we were able to compensate for the angular divergence of these beams and to collimate the output radiation to a single beam with a divergence of about 1 mrad.

As noted above, the generation of different frequencies in the active element is spatially separated, so that, using spatial modulation of the pump radiation, one can change the broadband lasing spectrum [10]. We placed in front of the input mirror a periodic mask (grid) with a shadow region of 80  $\mu\text{m}$  and its repetition period of 400  $\mu\text{m}$ . In this case, the output radiation represents a set of spectral lines (Fig. 4b) with a period equal to that of the mask multiplied by the spectral dispersion of lasing wavelengths in the active element. The maximum number of equidistant lines obtained with this mask was 15, covering the spectral range from 1.095 to 1.23  $\mu\text{m}$ .

To double the broadband lasing frequency, we used a nonlinear  $\text{LiIO}_3$  crystal 20-mm long with ends with anti-reflection coatings, cut for frequency doubling at 1.064  $\mu\text{m}$ . Matching of the angular synchronism dispersion and the

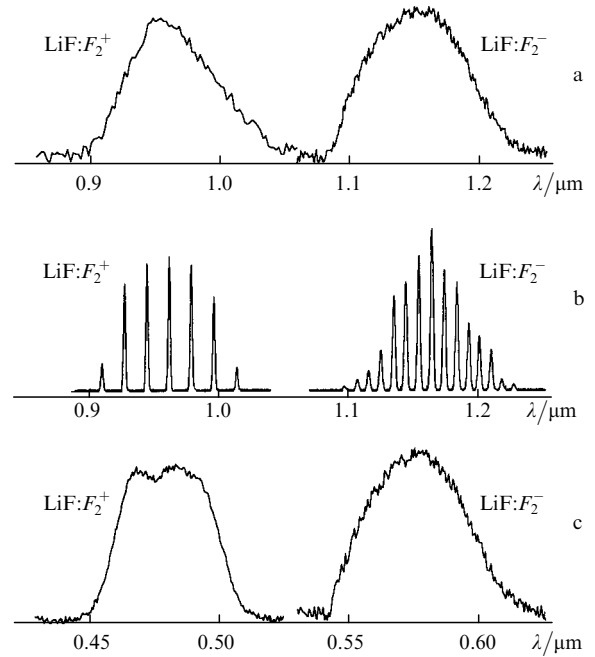


**Figure 4.** Spectra of pulses generated by  $\text{LiF:F}_2^+$  and  $\text{LiF:F}_2^-$  lasers in the broadband (a) and multifrequency (b) regimes, and the second-harmonic spectra of the broadband lasers (c).

spectral dependence of the angle of incidence of radiation on the nonlinear crystal was achieved using the spherical lens 7 with  $F_{2\omega} = 50$  mm. Selection of the proper angular magnification of the lens provided a 12% overall conversion efficiency of broadband infrared radiation to the second harmonic. The emission spectrum of the second harmonic in the visible (green–yellow–red) spectral region (0.545–0.615  $\mu\text{m}$ ) is shown in Fig. 4c.

Fig. 5 presents fragments of the second-harmonic emission spectra recorded in the multifrequency lasing regime at different pump pulse energies. The linewidth in the visible range was 0.38 nm for the pump energy  $E = 14$  mJ and 1.4 nm for the pump energy  $E = 25$  mJ. The increase in the linewidth can be explained by the increase in the inversion and gain, especially in the mask's half-shadow region, and by the increase in the SHG efficiency in the wings of the spectral lines.

Tight focusing of radiation into the nonlinear crystal provided not only the efficient frequency doubling but also

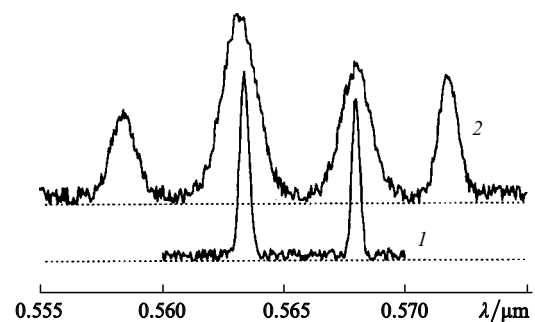


**Figure 5.** Fragments of the second-harmonic spectra of multifrequency lasing of the  $\text{LiF:F}_2^-$  laser for pump pulse energies equal to 14 mJ (1) and 25 mJ (2).

generation of the sum frequencies from various spectral regions of multifrequency lasing, which doubled the number of lines in the second-harmonic lasing spectrum (Fig. 6).

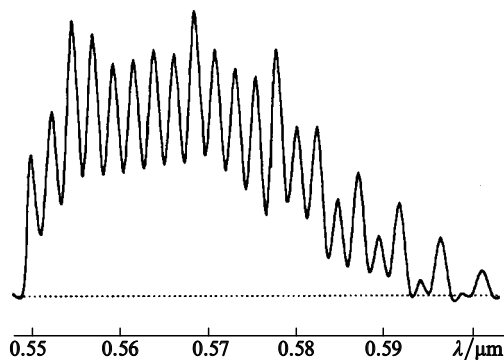


**Figure 6.** Emission spectrum of sum frequencies upon multifrequency lasing of the LiF: $F_2^-$  laser.

In this paper, we studied the emission from a broadband laser based on a LiF crystal with stabilised  $F_2^+$  colour centres [11]. The laser was excited by second-harmonic radiation ( $\lambda = 0.66 \mu\text{m}$ ) of a Nd<sup>+</sup>:YAG laser ( $\lambda = 1.32 \mu\text{m}$ ). The maximum pump radiation energy was 15 mJ at a pulse repetition rate of 10 Hz. The absorption coefficient of the investigated crystals at the maximum of the  $F_2^+$  band was  $K_{0.61} = 2.5 - 3 \text{ cm}^{-1}$ . The optical scheme of the cavity of the broadband laser was similar to that of the LiF :  $F_2^-$  laser. The intracavity lens had a focal length of 30 mm.

Upon excitation of the LiF :  $F_2^-$  laser by the pump laser at  $0.66 \mu\text{m}$  with a pulse energy of 12 mJ, broadband lasing in the  $0.89 - 1.04 \mu\text{m}$  region was observed (Fig. 4a). The maximum efficiency of the broadband laser amounted to 20% at  $E = 9 \text{ mJ}$  (Fig. 3). Spatial modulation of the pump radiation by a periodic mask resulted in the multifrequency lasing with the spectrum shown in Fig. 4b. The SHG efficiency of radiation from a LiF :  $F_2^+$  laser in a LiIO<sub>3</sub> crystal was 12%, and the broadband second-harmonic emission covered the blue-green spectral region from  $0.45$  to  $0.51 \mu\text{m}$ .

The broadband second-harmonic spectrum of a LiF :  $F_2^+$  laser is shown in Fig. 4c.

We also generated fourth harmonic from the broadband LiF :  $F_2^-$  laser. To do this, we used the BBO ( $5 \text{ mm} \times 5 \text{ mm} \times 10 \text{ mm}$ ) and KDP ( $15 \text{ mm} \times 15 \text{ mm} \times 30 \text{ mm}$ ) crystals. To achieve the ooe phase-matching after doubling, we employed a quartz  $\lambda/2$ -plate for  $\lambda = 0.575 \mu\text{m}$  to rotate the polarisation plane. The broadband second-harmonic emission was focused by a spherical lens with  $F_{2\omega} = 70 \text{ mm}$  into the nonlinear crystal. The maximum conversion efficiency to the fourth harmonic of visible light was obtained in the BBO crystal and reached 7%.

## 5. Conclusions

We demonstrated broadband and multifrequency lasing in LiF crystals with  $F_2^-$  and  $F_2^+$ -colour centres combined along with frequency doubling and quadrupling. The width of the lasing spectra amounted to  $0.13 \mu\text{m}$  in the region from  $1.1$  to  $1.23 \mu\text{m}$  for the LiF :  $F_2^-$  laser and  $0.12 \mu\text{m}$  in the region from  $0.9$  to  $1.02 \mu\text{m}$  for the LiF :  $F_2^+$  laser, while the

frequency conversion efficiency in these lasers was as high as 16 and 20%, respectively.

The matching of the spectral dependences of the angle of incidence of broadband radiation on the nonlinear crystal and of the phase-matching angle allowed us to achieve the efficient SHG in a nonlinear LiIO<sub>3</sub> crystal. Broadband and multifrequency radiation was generated in the  $0.55 - 0.615 \mu\text{m}$  region for the LiF :  $F_2^-$  laser and in the  $0.45 - 0.51 \mu\text{m}$  region for the LiF :  $F_2^+$  laser, with an overall conversion efficiency of 12%. Using the BBO crystal, we converted broadband visible radiation to the UV range with a 7% efficiency.

## References

1. Danailov M B, Christov I P *Opt. Commun.* **73** 235 (1989)
2. Basiev T T, Zverev P G, Fedorov V V *Tezisy Vsesoyuznoi Konferentsii 'Optika Lazero'* (Abstracts of Papers of the All-Union Conference on Laser Optics) (Leningrad: 1993), vol. 1, p. 79
3. Zverev P G, Basiev T T, Fedorov V V, Mirov S B *Proc. SPIE Int. Soc. Opt. Eng.* **2379** 54 (1995)
4. Basiev T T, Mirov S B *Room Temperature Tunable Color Center Laser* (Chur, Switzerland: Harwood Academic Press, 1994)
5. Basiev T T, Konyushkin V A, Mirov S B, Ter-Mikirtychev V V *Kvantovaya Elektron.* **19** 145 (1992) [*Sov. J. Quantum Electron.* **22** 128 (1992)]
6. Kogel'nik G, Li T, in: *Spravochnik po lazeram* (Laser Handbook) Ed. By A M Prokhorov (Moscow: Sovetskoe radio, 1978) Vol. 2, p. 21
7. Volosov V D, Kalintsev A Ya *Kvantovaya Elektron.* **3** 798 (1976) [*Sov. J. Quantum Electron.* **6** 434 (1976)]
8. Dmitriev V G., Gurzadyan G G, Nikogosyan D N *Handbook of Nonlinear Optical Crystals* (Berlin: Springer-Verlag, Springer Series in Optical Sciences, 1991), vol. 64
9. Basiev T T, Zverev P G, Papashvili A G, Fedorov V V *Kvantovaya Elektron.* **24** 591 (1997) [*Quantum Electron.* **27** 574 (1997)]
10. Basiev T T, Zverev P G, Fedorov V V, Mirov S B *Appl. Opt.* **36** 2515 (1997)
11. Basiev T T, Ermakov I V, Fedorov V V, Konyushkin V A, Zverev P G *Materialy konferentsii 'Tverdotel'nye perestraivaemye lazery'* (Proc. of Conf. on Solid-State Tunable Lasers) (Minsk: Institute of Molecular and Atomic Physics, 1994), p. 64